NIPPON STEEL & SUMITOMO METAL TECHNICAL REPORT No. 119 SEPTEMBER 2018

Technical Report

UDC 621 . 791 . 763 . 3 . 016 : 621 . 384

Development of Laminar Plasma Shielding HF-ERW Process

Hideki HAMATANI*
Fuminori WATANABE
Sunao TAKEUCHI
Takuya ASANO
Noboru HASEGAWA
Nobuo MIZUHASHI
Tetsuro NOSE
Takao MIURA

Abstract

The shielding technique for high frequency-electric resistance welding, HF-ERW, is considered a key factor in the formation of a sound weld. Compared to the cold gas shielding technique, high temperature gas shielding, due to its higher kinetic viscosity coefficient, should make it easier to sustain a higher laminar flow, thus leading to low air entrainment in the shielding gas. In addition, plasma is in a much higher temperature state > 5 000 K, and the dissociated gases can react with the entrained oxygen; plasma jets should, therefore, enhance the overall shielding effects. We have developed a plasma torch that can generate a long and wide laminar argon-nitrogen-(hydrogen) jet, and then confirmed its shielding effect through pipe forming tests of carbon steel, a yield strength grade of X65, as well as high-Cr steels containing easily oxidized elements. Preliminary attempts at applying this novel shielding technique have, as expected, demonstrated extremely low numbers of weld defects and a good low temperature toughness of the HF-ERW seam.

1. Introduction

Electric resistance welded (ERW) steel pipes are used in a wide variety of industrial fields such as energy and automobiles; their advantages as an industrial material include economical price, good roundness, and excellent shape properties such as uniform wall thickness, and as a result, they have high crushing resistance, expandability, and good girth weldability. The conventional weld seam produced by HF-ERW, on the other hand, often has a relatively low toughness due to the forming oxide defects in the weld seam during welding. In view of the problem, we have studied the welding mechanisms, and on the basis of the findings, developed techniques for monitoring and controlling welding heat input[1–5], making it possible to produce ERW pipes with sound seams. Regarding ERW pipes of stainless steel containing easily oxidized elements such as Cr, Si, etc. in large amounts, gas shielding of the seam welding is essential.

Box type shields are often used to minimize the oxidation at the ERW joint; they, however, have disadvantages such as that shield boxes of different sizes have to be used for different pipe diameters, and that scale accumulating in the box may get into the joint to form defects. As a solution, some reports propose the blowing of inert gas at room temperature as a shielding medium not requiring boxes[6, 7]. In this case, the blown gas tends to be turbulent, draws in the atmosphere, and as a result, the oxygen potential in the shield gas flow is not always low. Compared to the cold gas shielding technique, high temperature gas shielding, due to its higher kinetic viscosity coefficient, should make it easier to sustain a higher laminar flow, thus leading to low air entrainment in the shielding gas[8–10].

2. Plasma as Shielding Medium

As a shielding medium, plasma has advantages such as: (1) it easily forms a laminar flow and negligibly entrains the atmosphere; (2) even when the atmosphere is drawn in, atoms in the plasma react with oxygen to lower the oxygen concentration; and (3) oxides are melted and water causing oxidation is removed by the high temperature. These advantages are explained below in detail.

According to the kinetic theory of gas molecules, the dynamic coefficient of viscosity μ is expressed as follows:

$$\mu = \left(\frac{T}{T_0}\right)^{\frac{3}{2}} \frac{T_0 + S}{T + S}\,\mu_0 . \tag{1}$$

* General Manager, Head of Material Properties Evaluation Div., ph.D, Nippon Steel & Sumikin Technology Co., Ltd.
20-1 Shintomi, Futtsu City, Chiba Pref. 293-0011
(Former General Manager, Head of Div., ph.D, Nagoya R & D Lab.)

Table 1 Power low viscosity parameter for gases[11]

	T_0 (K)	μ_0 (Ns/m²)	n	S
Ar	273	2.13E-05	0.72	144
N_2	273	1.66E-05	0.67	107
H_2	273	8.41E-05	0.68	97

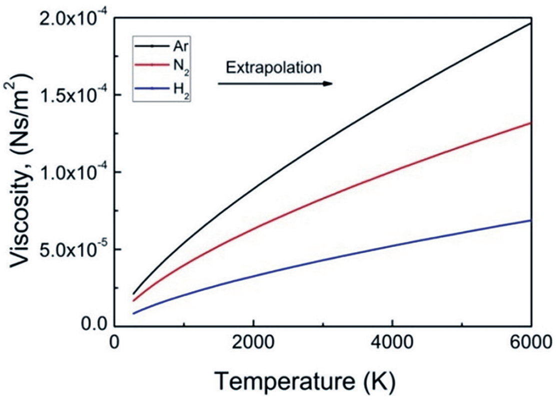

Fig. 1 Estimated gaseous viscosity

Then, using the viscosity parameters of Ar, N_2 and H_2 given in **Table 1**,[11] their dynamic viscosity figures at different temperatures are calculated as shown in **Fig. 1**; with an increase in temperature, the viscosity increases.

The Reynolds' number Re, an indicator of the degree of turbulence of a flow field, is expressed as

$$\mathrm{Re} = \frac{\rho VD}{\mu}\ , \tag{2}$$

Where ρ is the gas density, V is the flow velocity, and D is the characteristic length. The higher the gas temperature, which means higher viscosity, the smaller the Reynolds' number that will be achieved. This means that it is easier with gas at high temperature to obtain a laminar flow because of the higher dynamic coefficient of viscosity than at room temperature. Since a plasma jet more than 5000 K is expected to form a laminar flow easily[12], it is more suitable as a shielding medium than a turbulent gas, which easily draws in the surrounding atmosphere.

In addition, when multi-atom molecules are used for the plasma, dissociated or ionized atoms (X) and positive ions (equation (3)) react with drawn-in oxygen (see equation (4)), and as a result, the oxygen concentration inside the shielded zone is expected to be very low:

$$X_2 \rightarrow 2X\ , \tag{3}$$

$$2X + O_2 \rightarrow 2XO\ . \tag{4}$$

Another advantage of high-temperature gas such as thermal plasma is that high-melting point oxides and water vapor, causing oxidation, on the joint surfaces are possibly melted, vaporized and dissipated. Since such oxides on the joint surfaces and scales and spatters entering the joint cannot be shut out by the shielding, it is necessary to render them harmless by upsetting, that is, by melting and squeezing them out of the joint together with molten steel. Assuming that the oxides are spherical, the time t_s it takes to completely melt an oxide particle is expressed as follows:

$$t_s = \frac{\rho_s rC}{M\alpha}\log\frac{T - T_{in}}{T - T_{mp}} + \frac{\rho_s rq}{M\alpha(T - T_{mp})}\ . \tag{5}$$

Here, ρ_s is the specific density, r is the diameter, C is the heat capacity, M is the molecular mass, q is the latent heat of fusion, T_{in} is the initial temperature, and T_{mp} is the melting point of the particle in question, T is the gas temperature, and α is the thermal conductivity of the plasma. In equation (5), the second term on the right side is smaller than the first.

For example, a particle of Al_2O_3, 50 μm in diameter, is completely melted when heated in an Ar plasma at 4000 K for 6 ms. By using an Ar-N_2-(H_2) plasma, having a higher thermal conductivity than that of Ar, larger particles can be melted within the same time period.

In consideration of the above, we embarked on the development of a new shielding method for ERW using an inert plasma jet of Ar-N_2-(H_2) at high temperature.

3. Problems of Conventional Plasma Torches

When a plasma jet of the transfer type like that for tungsten inert gas (TIG) welding is used for the shielding of ERW joints, the plasma may become unstable because the steel material, which acts as an electrode, travels at tens of meters per minute. As for non-transfer type torches, on the other hand, DC (Direct Current) torches, which are often used for thermal spraying, etc., are available in the market. In this case, because plasma is formed by applying a voltage between the anode and cathode, the travel of the pipe at high speed does not adversely affect the stability of the plasma. The conventional plasma jet of this type of torch, however, is turbulent, and it is difficult to obtain a high-temperature portion of the jet extending longer than five to seven times the nozzle inner diameter (ID, usually as small as 10 mm or less)[13], which means that the maximum plasma length obtainable is 100 mm or less. Due to this short plasma, the torch will interfere with the equipment around the welding point of the pipe mill.

When the torch diameter is large, the plasma jet tends to be unstable. To solve this problem and stabilize the plasma jet, it is effective to use an axially tangential gas flow, so as to rotate anode spots on the anode surface. However, increasing the flow amount of the tangential gas means greater turbulence disturbing the desired laminar flow, and is inadequate for the purpose of shielding. In this relation, a method has been developed whereby a solenoid is provided around the circumference of the anode, and the rotation of anode spots is controlled by the electromagnetic force. In this case, however, the torch structure will be complicated and its size too large to fit into the congested space near the seam welding position.

In addition, the conventional turbulent plasma jets generate huge noise, using H_2 gas as the working gas, the noise, especially, sometimes exceeds 120 dB, and is therefore inadequate for application to production plants.

As stated above, developing a new type of torch capable of forming a plasma jet comparatively large in diameter, tolerable in noise emission and entraining the atmosphere only in a small amount was essential for obtaining the intended shielding effect and commercial production of ERW pipe taking advantage of the effect.

4. Development of Laminar-flow Plasma Torch and Its Characteristics

Figure 2 schematically shows the structure of the developed laminar-flow plasma torch. It is characterized by the cascade composed of the inter-electrode inserts (IEIs), insulated from each other; it electrically insulates the anode from the cathode, and keeps them away from each other by about 100 mm[14–16]. Plasma torches available in the market lack this cascade portion, and the anode-cathode distance is less than 10 mm.

Kolmogorov's law states that the turbulent motion of a gas flow decreases as a result of the dissipation of vortex energy, and the plasma jet flow changes to laminar along its flow. Accordingly, it is possible with the developed plasma torch to decrease the turbulence of the jet as it flows towards the anode, and form a laminar flow at the exit nozzle. In fact, the visible plasma length increases as the anode-cathode distance increases (see **Fig. 3**), which corroborates the said law.

In addition, it has been found that, in obtaining a laminar flow with a plasma torch, there are many influencing factors related to the torch structure. For example, the torch diameter profile from the cathode to the anode and the spread angle of the cathode significantly affect the plasma flow mode. **Figure 4** is an example study map showing the relationship between the IEI profile and a plasma jet in a laminar flow. The cascade is composed of a plurality of IEIs of the same length (L) and different ID (see Fig. 2), and when the number of IEIs of the same ID part number increases, the torch inner space of the same diameter grows longer. In Fig. 4, by using this length to be referred to as the uniform length, L, and the step, Δr, as the difference ID between adjacent IEIs, "the high temperature portion" (here, determined as "visible plasma length") is evaluated in relation to the ratio of step, Δr/L. It is clear from the figure that, in order to obtain a plasma length of 500 mm or longer, for example, it is necessary to set the Δr/L at roughly 1/5 or less. The possible primary reason for the result is that the re-torch of the jet within each step surface of the IEI sustains the plasma stability.

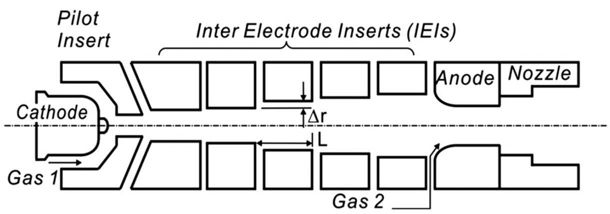

Fig. 2 Cutaway views of cascade torch

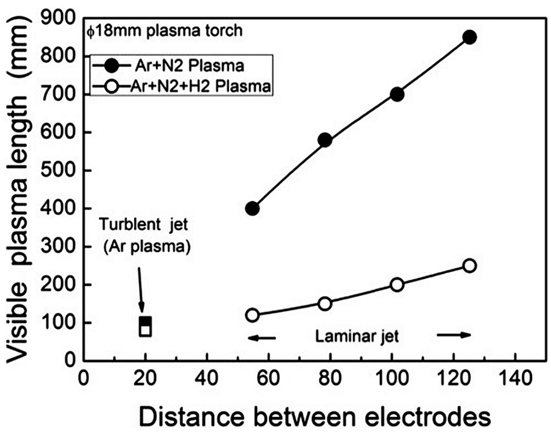

Fig. 3 Effect of distance between electrodes on visible the plasma length

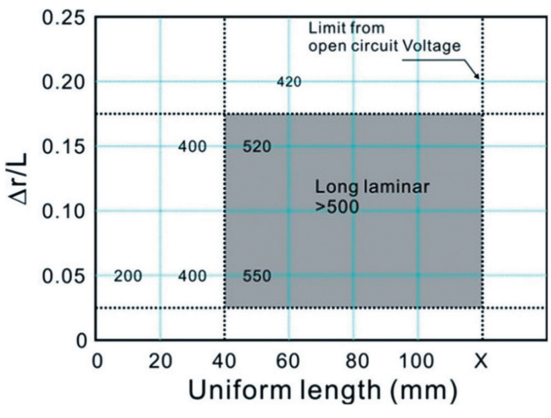

Fig. 4 Effect of IEI profile on the plasma length (Ar-N_2)

Furthermore, the component mixing ratio of the plasma gas was found to affect the flow mode. In fact, it was easier to obtain a laminar flow using N_2 as the main gas than Ar, because of the lower density of N_2, as is understood from equation (2).

Figure 5 compares the plasma jet of the developed torch with that of a commercially available torch; the torch used here was 2086A made by Praxair. Discharge conditions from various plasma torches are similar, but not exactly identical. These photographs are useful for identifying visible plasma length, the white portion, in the plasma jet. The visible plasma length of the commercial torch is at least 100 mm, since the plasma is turbulent and rapidly cooled by the entrained air. In contrast, the developed torch proved capable of forming a plasma jet having a visible plasma length, about 20 mm in diameter, is over 500 mm. It has to be noted that the shielding of the ERW seam, which will be presented later herein, does not utilize the turbulent tail portion of the jet more than 500 mm from the nozzle exit but its core portion 100 to 300 mm from it.

In addition, in the case of the laminar plasma, the irradiation distance must be set longer; therefore, the plasma torch set position around the welding point of the pipe mill must be moderated in the case of the turbulence.

Assuming an asymmetric 2D model for the plasma jet geometry and a plasma gas with 10% H_2 in addition to the above, the radial distribution of oxygen partial pressure in turbulent and laminar-flow plasma jets was calculated by combining the Fluent standard κ-ε model and combustion theories; here, regarding the reactions of the plasma components, only molecular dissociation and oxidation were taken into consideration, also, int case of laminar plasma flow, by selecting minimum κ and ε values, the turbulence was overestimated. The calculation of the oxygen partial pressure at the center of the jet at 150 mm from the exit of the torch result is given in **Fig. 6**. This figure illustrates that the choice of the plasma torch significantly influences the oxygen content field. When the flow is turbulent, it is roughly a half that in the atmosphere; in contrast, when the flow is laminar, it may enhance by four to five orders of magnitude.

Figure 7 shows the measurement result of the temperature distribution in the axial direction of a plasma jet in a laminar flow obtained through optimum combination of the anode-cathode distance, gas composition, IEI profile, etc.; the line pair method using the luminescence intensity ratio of Hα and Hβ was employed for the measurement. There is a long high-temperature portion at approximately 5 000 K extending to roughly 200 mm from the torch exit in a temperature gradient as shallow as 20 K/mm, approximately.

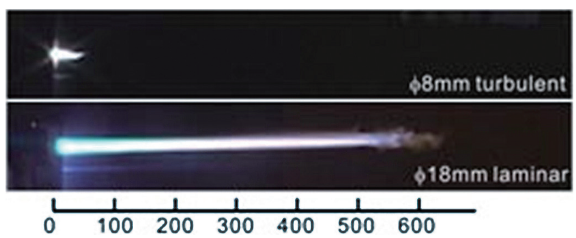

Fig. 5 Comparison of plasma jets

As for the effect of the anode-cathode distance over the voltage, another property item of a plasma torch, the two were found to be proportionate to each other as shown in **Fig. 8**; the plasma resistance was roughly 0.8 V/mm with pure Ar, and 1.4 V/mm with $18N_2+3Ar$. The resistance with pure Ar was slightly lower than that in common TIG welding; this is presumably because the gas density was low. In either of the cases, the total voltage drop of the two electrodes was constant at roughly 40 V.

It has to be noted in relation to the above that, from Fig. 3, when the plasma working gas is $Ar\text{-}N_2\text{-}H_2$, the plasma becomes shorter because of the plasma pinching force due to the high energy required for turning H_2 into plasma, and that, from Figs. 3 and 8, to obtain a visible plasma length of $Ar\text{-}N_2$ roughly 500 mm in length, a voltage nearly as high as 200 V is required, and to stabilize the plasma, a power source unit having high no-load resistance is necessary.

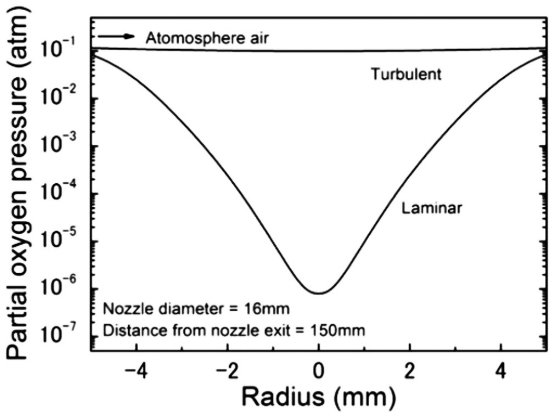

Fig. 6 Calculated radial distribution of oxygen partial pressure in turbulent and laminar plasma jets (10% hydrogen content, 16 mm nozzle inner-diameter, at 150 mm from nozzle)

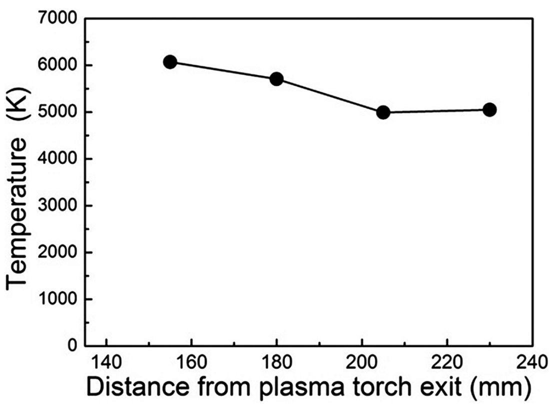

Fig. 7 Axial temperature profile of $Ar\text{-}N_2\text{-}H_2$ plasma of cascade torch (18 mm nozzle inner-diameter, ID)

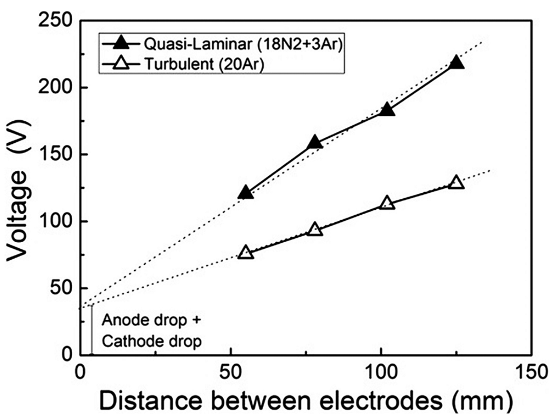

Fig. 8 Effect of electrodes distance on the voltage between electrodes

5. Effects of Plasma Shielding

5.1 Test method

The effect of plasma shielding to reduce ERW defects was evaluated in laboratories using a torch made by us and a commercially available one (2086A made by Praxair). **Figure 9** shows the outlines of the test equipment. Two steel plates of JIS SUS304, 6 mm in thickness, simulating the plate edges to weld, were placed in contact with power-supply shoes and transferred at a prescribed speed, heated by a high frequency power supply, and welded by ERW under upsetting and the plasma shielding at the welding zone. As illustrated, the plasma jet was irradiated from the torch provided between the contact shoes to the area around the welding point. In Fig. 8, V_0 is the welding point, and V_p is the target point for the plasma irradiation.

The width (A_w) and length (A_l) of the area along the welded seam covered by the plasma jet are expressed using the diameter (D_p) of the jet as follows:

$$A_w \geq D_p\,; \quad (6)$$

$$A_l \geq D_p/\sin\theta\,,\quad (\theta \approx 10-30)\,. \quad (7)$$

Here, θ is the angle of the plasma irradiation. The welding speed was assumed to be constant at 30 m/min, and oxidation of the welded joint to be caused by the atmosphere and the water supplied through tubes, 4 mm in inner diameter, at a rate of 0.8 l/min each. The test parameters were the input power for the ERW, the use or otherwise of the shield, the target point of the shielding jet irradiation (or, the distance between V_0 and V_p), the degree of laminar flow of the plasma jet (controlled by changing the gas composition and the flow amount), etc. The welded joints thus obtained were evaluated in terms of defect area ratio (the area of penetrators and cold defects /total joint area) at fracture observation after the Charpy test at 160°C. The reason for the Charpy test temperature of 160°C is that the failures other than those caused by oxides exhibit ductile fracture surfaces at this temperature, and the defective area can be distinguished easily.

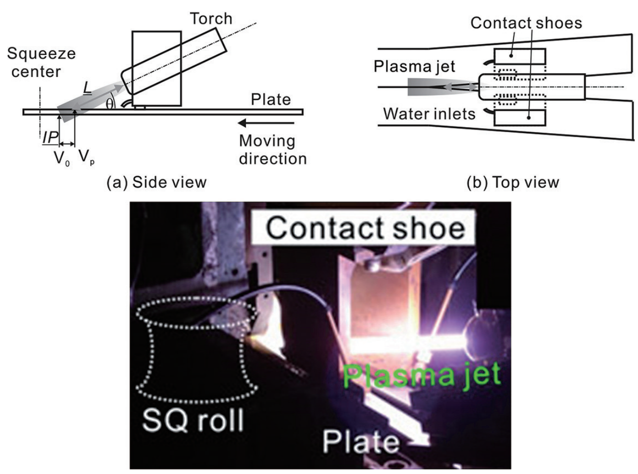

Fig. 9 Experimental setup highlighting the plasma shielding HF-ERW process

5.2 Test results and discussion

In the first place, **Fig. 10** shows the relationship between the input power for ERW and the defect area ratio of the joint obtained with shielding by the commercially available torch, 8 mm in anode ID. The figure shows that, in the case of the conventional HF-ERW without plasma shield, the defect area ratio was around 0.3% under the most adequate input power condition. A lower power condition results in the cold defects owing to insufficient heating. For larger power, excessive molten metal was observed to be the cause of penetrators.

On the other hand, when the ERW was performed under an adequate input power condition and shielding with an adequate irradiation point, the defect area ratio was as low as 0.01% or less. This value is considered to be lower than the oxide inclusion ratio in the base metal. However, by shifting the plasma irradiation point to be 10 mm (Best-10 in the graph), this enhancement could not be observed. A possible explanation of this outcome is that, during welding, the effective ID was as small as 8 mm, and the shield area was out of its coverage. Taking these results into consideration, we have developed a plasma torch of a larger anode ID and evaluated its effect of enhancing the robustness of the shielding effect.

Figure 11 shows the shielding effect of the plasma jet of the developed torch in a laminar flow and 18 mm in ID. As expected, an increase in the plasma diameter drastically increased the irradiation point tolerance, and the effect was substantially unchanged even when the irradiation point of the developed torch shifted by 10 mm or more.

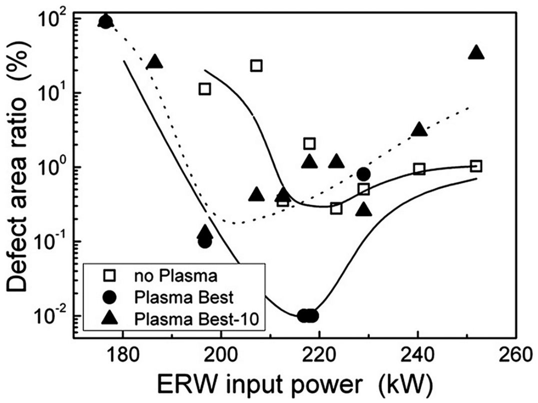

Fig. 10 Shielding effect of Ar-H_2 turbulent plasma with commercial torch on the weld defect reduction (8 mm ID, material SUS304)

A shielding effect of hydrogen gaseous addition as plasma working gas on the weld defect area ratio is shown in **Fig. 12**. Under the most adequate power input condition, the defect area ratio decreased with the plasma shielding using either Ar-N_2 gas or Ar-N_2-H_2 gas. Although the hydrogen gas is not always necessary, the shielding enhancement of the Ar-N_2-H_2 plasma system is often superior to that of the Ar-N_2 system. It has to be noted here that, with both of the two gas systems, the defect area ratio increased for an ERW input power. This is presumably because the welding point (V_0) shifted to outside the shielded area as the power input changed. To further improve the robustness of the shielding effect, therefore, it is necessary to control the target point (V_P) of the plasma jet so as to follow the move of V_0.

5.3 Verification test on commercial ERW line

A preliminary attempt at applying this novel shielding technique to pipe line production was conducted at the Nagoya 16 inch mill. A high strength line pipe with a yield strength of X65 grade was employed in this study. **Figure 13** (a) (b) illustrates the effects of the shield with a laminar plasma jet of Ar-N_2 gas as evaluated in terms of the defect area ratio.

Under normal ERW conditions, the weld defect area ratio is minimized at an adequate input power range where the defect area ratio of the joint is below 0.05% (equal to the base metal); however, this range is as narrow as 10% or less of the total input power control range. It was clear, on the other hand, that by the laminar plasma shield, the width of the adequate input power range was almost doubled.

It is also expected that the defect area ratio and cross sectional microstructure will directly affect the toughness of the welds and as such, the absorbed energy value is determined from Charpy impact testing. In a comparison of the absorbed energy of the weld seam, in Fig. 13 (b), via the Charpy test with a thickness of 7.5 mm is converted to the full size value, which is multiplied 10/7.5 to the measure value. On the assumption that the absorbed energy is proportional to the thickness, at a fixed ERW input power, demonstrating that it is possible to improve ductile-brittle transition temperature, vTrs, by approximately 20°C, owing to the decrease of defects.

Furthermore, another plasma shielding enhancement for steel containing easily oxidized Cr by 13%, using a plasma gas with H_2, has proved effective at decreasing the defect area ratio by one order of magnitude or more (see **Fig. 14**). In consideration of the fact that, in the laboratory tests on SUS304 and 13Cr steels described earli-

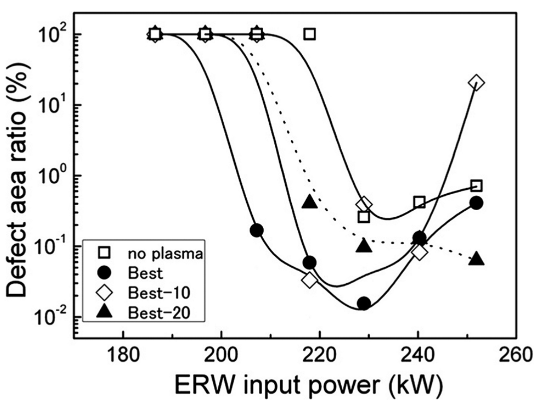

Fig. 11 Shielding effect of Ar-N_2-H_2 laminar plasma with developed torch on the weld defect reduction (18 mm ID, material SUS304)

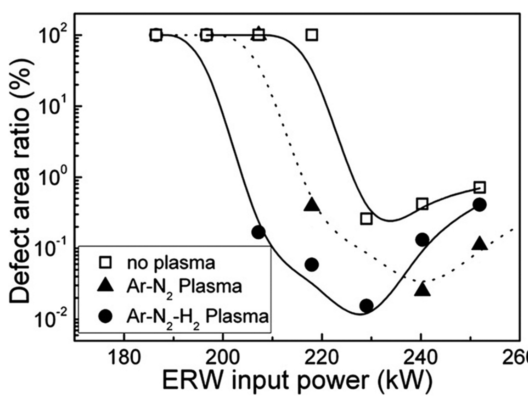

Fig. 12 Defect reduction effect of hydrogen addition to plasma shielding gas (18 mm ID, material SUS304)

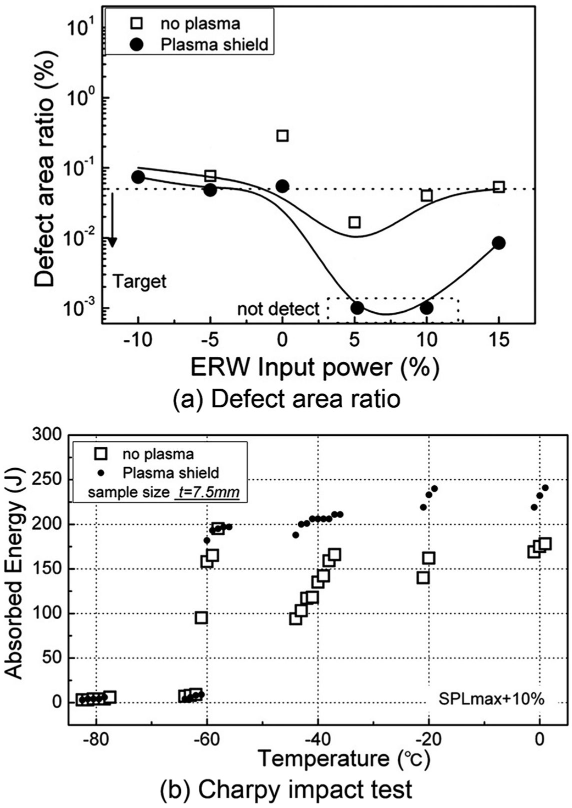

Fig. 13 Enhancement of plasma shielding on commercial ERW line (material API-X65)

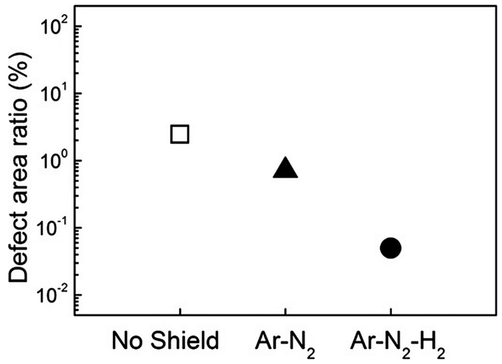

Fig. 14 Enhancement of plasma shielding on commercial ERW line (material 13Cr steel)

er[17)], Ar-N_2 gas produced better results than the above test on X65, weld defects can be decreased even further by optimizing the aiming of the plasma irradiation point.

5.4 Development of plasma aiming control

As stated above, penetrators are greatly decreased and the Charpy impact properties improved by the plasma shield when the plasma jet is adequately targeted to cover the welding point. In order to fully enjoy this effect, however, it was necessary to align the axle of the plasma jet to the seam welding line. We focused attention on the already-developed heat input control and welding monitoring technique, and utilized them for that purpose.[5)] By the welding monitoring technique, using a color CCD camera, however, the Planck radiation from the heated steel and the light emission of the plasma were determined to be at the same intensity level, and because of their mutual interference, it was impossible to measure their relative position by image processing.

To solve the problem, wavelength separation of the Planck radiation and the plasma light was proposed. The wavelength components up to 1 μm and those exceeding 1 μm were separated from each other based on the Planck radiation at different temperatures given in **Fig. 15**(a) and the bright line spectra of the plasma gas components, namely Ar, N_2 and H_2 (from the NIST data base). Based on this, a photographing system was developed, whereby near infrared components and specific blue components of the lights were separately captured by using two high-sensitivity CMOS cameras with special optical filters. Thanks to this method, images of the Planck radiation from the steel plates to the weld and the plasma jet were obtained independently from each other, and after working out the algorithms for image processing of the two, it became possible to separately detect the plasma jet centerline and the welding line (see **Fig. 16**). On this basis, a mechanism has been developed for controlling the mounting robot arm for the plasma torch so that the plasma axle is automatically aligned to the welding line.

6. Conclusion

A cascade type plasma torch capable of forming an Ar-N_2 jet having a visible plasma length of more than 500 mm and a diameter of about 20 mm has been developed. The plasma jet in a laminar flow from the developed torch has been used for shielding the welding point of ERW pipes of JIS SUS304, and proved effective at decreasing the defect area ratio of the welded seam by an order of magnitude or more. When this shielding technique was applied to the production of API X65 class pipes, the defect area ratio and vTrs were markedly improved. These results point to the possibility of producing ERW pipes of higher reliability than was conventionally

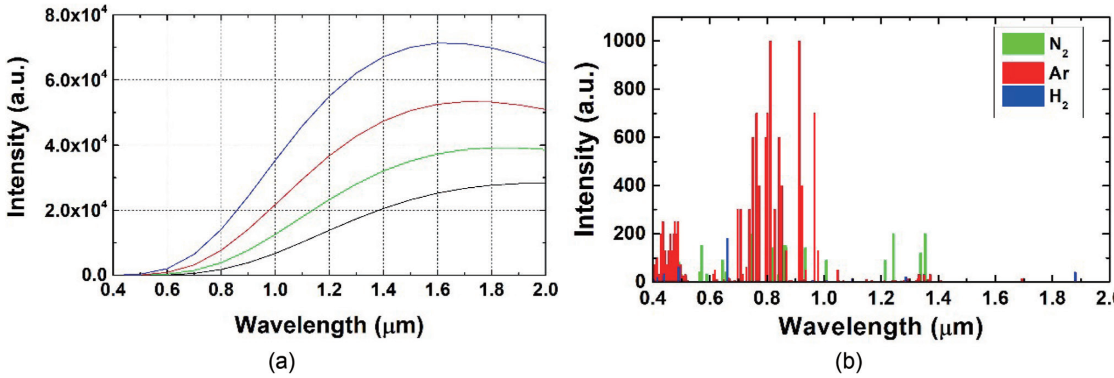

Fig. 15 Planck radiation and spectra of Ar, N_2 and H_2

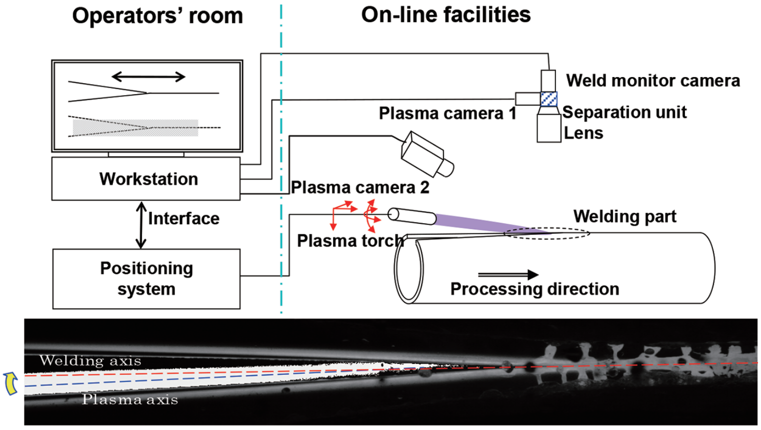

Fig. 16 Automatic positioning system of the plasma jet direction

possible.

Acknowledgements

We would like to express our sincere gratitude to Prof. Oleg P. Solonenko, Dr. Andrey V. Smirnov and related people of ITAM (the Institute for Theoretical and Applied Mechanics) of the Russian Academy of Sciences for their valuable support in the development of the laminar-flow plasma torch of the present study.

References

1) Haga, T. et al.: Research Supplement. The Welding Journal. July, 208 (1980)
2) Haga, T. et al.: Research Supplement. The Welding Journal. July, 104 (1981)
3) Fukami, T. et al.: Proc. Int. Pipeline Conf. 2012. Vancouver, 2012, p. 229
4) Hasegawa, N. et al.: Proc. Int. Pipeline Conf. 2012. Vancouver, 2012, p. 237
5) Hasegawa, N. et al.: Proc. International Ocean and Polar Engineering Conf. 2017. San Francisco, 2017, p. 107
6) Nichols, R. K. et al.: Practical Welding Today, March/April, 29 (1988)
7) Fukuda, Y. et al.: Sumitomo Metal Industries Ltd. September, (1992)
8) Hamatani, H. et al.: Preprints of the National Meeting of JWS. 2011f, 2011, p. 376
9) Hamatani, H. et al.: CAMP-ISIJ. 715 (2012)
10) Hamatani, H. et al.: Proc. International Ocean and Polar Engineering Conf. 2012. Vancouver, 2012, p. 246
11) Hilsentrath: Table of Thermodynamic and Transfer Properties, Nat. Bur. Std. Circular. Pergamon, 1960, 564p
12) Boulos, M. I. et al.: Thermal Plasma. Plenum Press, 1994, 269p
13) Chen, X.: Pure Appl. Chem. 78 (6), 1253 (2006)
14) Kuz'min, V. I. et al.: Proc. of the 8th National Thermal Spray Conference. Houston, 1995, p. 83
15) Solonenko, O. P. et al.: HTPP9. Abst. Petersburg, 2006, p. 10
16) Osaki, K. et al.: Vacuum. 59, 47 (2000)
17) Watanabe, F. et al.: Proc. International Ocean and Polar Engineering Conf. 2017. San Francisco, 2017, p. 447

Hideki HAMATANI
General Manager, Head of Material Properties Evaluation Div., ph.D
Nippon Steel & Sumikin Technology Co., Ltd.
20-1 Shintomi, Futtsu City, Chiba Pref. 293-0011
(Former General Manager, Head of Div., ph.D
Nagoya R & D Lab.)

Sunao TAKEUCHI
Former Nippon Steel & Sumikin Research Institute Corporation

Noboru HASEGAWA
Chief Researcher, ph.D
Nagoya R & D Lab.

Tetsuro NOSE
Director, Member of the Board, Dr.Eng.
Welding Machinery & Eng. Unit
Plasma Welding Machinery & Eng. Unit
Optical Fiber & Eng. Unit
Nippon Steel & Sumikin Welding Co.,Ltd.

Fuminori WATANABE
Researcher
Nagoya R & D Lab.

Takuya ASANO
Manager, Head of Pipe & Tube Section
Pipe & Tube Mill
Pipe & Tube Div.
Nagoya Works

Nobuo MIZUHASHI
Former Pipe & Tube Research Lab.
Steel Research Laboratories

Takao MIURA
Director, General Manager
Wuxi Nippon Steel & Sumikin Pipe Co., Ltd.